sustainability

MDPI

Article

Organic–Inorganic Nanocomposites of *Aspergillus terreus* Extract and Its Compounds with Antimicrobial Properties

Ibrahim Seyda Uras [1,2], Baris Karsli [3], Belma Konuklugil [1,4], Ismail Ocsoy [5] and Ayse Demirbas [3,*]

[1] Department of Pharmacognosy, Faculty of Pharmacy, Ankara University, Ankara 06560, Turkey
[2] Department of Pharmacognosy, Faculty of Pharmacy, Agri Ibrahim Cecen University, Agri 04100, Turkey
[3] Department of Seafood Processing Technology, Faculty of Fisheries, Recep Tayyip Erdogan University, Rize 53100, Turkey
[4] Department of Pharmacognosy, Faculty of Pharmacy, Lokman Hekim University, Ankara 06510, Turkey
[5] Department of Analytical Chemistry, Faculty of Pharmacy, Erciyes University, Kayseri 38039, Turkey
* Correspondence: ayse.demirbas@erdogan.edu.tr; Tel.: +90-464-2233385-1440

Abstract: Due to its distinct, atypical features and possible applications, three-dimensional (3D) hierarchical nanoflowers have sparked considerable interest. Copper (II) ions were employed as inorganic components in this study, whereas various extracts from *Aspergillus terreus* and their extracted main components were used as organic components. Extracts from *A. terreus* and its isolated principal component molecules can first form complexes with copper ions, and these complexes subsequently become nucleation sites for primary copper phosphate crystals, showing interactions using an easy and successful self-assembly template synthesis technique. Therefore, the process results in the formation of 3D nanoflowers among the *A. terreus* extract and its remoted important additives in addition to copper ions, ensuing in a completely unique round flower-like shape containing loads of nanopetals under the most excellent conditions along with pH, attention of organic–inorganic additives, temperature, and the quantity of copper nitrate on nanoflower formation. Furthermore, *A. terreus* and its isolated major components, $Cu_3(PO_4)_2$ nanoflowers, seemed to have a remarkable antibacterial effect. Our findings highlight the benefits of nanoflowers made with *A. terreus* and its isolated secondary metabolites of inorganic structures, which could be used in industrial biocatalysts, biosensors, and environmental chemistry.

Keywords: *Aspergillus terreus*; nanoflowers; antimicrobial; hybrid nanocomposites

Citation: Uras, I.S.; Karsli, B.; Konuklugil, B.; Ocsoy, I.; Demirbas, A. Organic–Inorganic Nanocomposites of *Aspergillus terreus* Extract and Its Compounds with Antimicrobial Properties. *Sustainability* **2023**, *15*, 4638. https://doi.org/10.3390/su15054638

Academic Editor: Konstantinos S. Triantafyllidis

Received: 3 December 2022
Revised: 16 February 2023
Accepted: 3 March 2023
Published: 5 March 2023

1. Introduction

Seas and oceans comprise a wide diversity of species with biologically active secondary metabolites that have been proven to be rich and promising sources of new and novel bioactive natural products with potential pharmaceutical significance.

During the search for new drug sources for the treatment of different diseases, marine natural compounds have been found to play an important role in directing drug discovery research. For this reason, the research studies in this area have been increasing extensively in recent years [1].

Along with the diseases that have changed over time, the active ingredients of drugs used in the treatment of diseases also change. As a result of the incorrect use of antibiotics, the existence of drug-resistant microorganisms has become one of the biggest public health problems today. Among the drugs needed for public health, new antimicrobial drugs targeting bacteria and fungi resistant to existing antimicrobials are at the top. The fact that more than half of the antibiotics approved by the FDA are natural or derived from natural compounds shows that natural sources are important for the search for new antibiotic-active substances [2].

Discovery efforts of bioactive natural compounds have shifted from terrestrial sources to marine sources. Because of the extreme, unusual, and compelling environmental factors

of the marine habitat, organisms, such as sponges, corals, algae, etc., produce different secondary metabolites to the outcome of these challenging conditions. More than 50% of identified marine natural compounds are only isolated from marine sources. Similar to marine organisms, marine fungi also adapt themselves in marine habitats by producing a variety of secondary metabolites, which is not seen in their terrestrial counterparts. Marine fungi can be found in all marine habitats and can be isolated from many different sources. Endophytic fungi cohabiting with marine organisms are a valuable candidate for a sustainable drug discovery process. Numerous new compounds have been isolated from many marine organisms. In the case of uncontrolled collection of marine organisms for secondary metabolite isolation, some species will be ecologically endangered, as evidenced in terrestrial samples. Marine fungi overcome these concerns and are a sustainable source of active substances. Yield enhancement of the desired metabolite through media manipulation, biotic and abiotic elicitors, incubation interval, genetic engineering approaches, etc., can be achieved. When the activities of marine-derived compounds were examined, it was determined that the antimicrobial activity was the second most observed activity with 13% after the anticancer activity [3].

Fungi from marine sources are significant sources of bioactive compounds for the drug discovery process. Together with cephalosporins, one of the most famous examples of bioactive compounds, marine fungi have been shown to offer unique chemicals of clinical significance [4]. Marine-derived fungi have produced a number of substances with unusual chemical structures and bioactivity [5,6]. Many compounds with various bioactivities, such as anticancer, antibacterial, anti-inflammatory, antidiabetic, antiviral, antioxidant, antifungal, and antimycobacterial activity, have been obtained from marine-derived *A. terreus* fungus in different studies [7]. Butyrolactone I has significant antimycobacterial activity [8], potent antifouling activity [9], and significant inhibitory activity against α-glucosidase [10], while butyrolactone III shows significant antioxidant activity [11]. Several plant extracts and active compounds are used in the production of metallic nanoparticles as organic reducing and stabilizing agents [12,13]. Antimicrobial activity of butyrolactone I derivates from *Aspergillus terreus* and has been reported against various Gram-positive and Gram-negative bacteria as well as fungi [14]. The antimicrobial effects of the compounds can be further enhanced by synthesizing them with silver nanoparticles. Significant antibacterial activity of AgNPs at different concentrations synthesized using *A. terreus* was reported against all bacterial strains tested, and it was also reported that the antimicrobial activity of these AgNPs differed according to the concentration and bacterial species [15]. The antimicrobial effects of extracts differ according to various factors, such as extract method, concentration, and tested bacteria. Additionally, the high phenolic and flavonoid content in the extracts may also affect the antimicrobial activity [16]. Therefore, it is extremely important to identify compounds with higher antimicrobial properties and apply them in various fields such as including pharmaceuticals, food preservation, natural therapies, and alternative medicine.

Nanodendrites [17–19], core–shell nanoparticles [20–22], nanobullets [23–25], nanotubes [26–29], nanowires [30–33], nanozymes [34–39], and nanoflowers [40–45] have received a lot of attention, and significant progress in this area of research has been achieved in recent years. "Nanoflower" is a great term for certain nanomaterials with microscopic images that resemble flowers. Carbon [46–48], metals and other elemental materials [49–51], alloys [52,53], and metaloxides/hydroxides [54–56] are among the materials that have been observed to produce "flower-like formations" [57–61]. These nanoflowers have an extensive variety of applications in catalysis, magnetism, nanodevices, sensing and biosensing, and medicine because of their enormous surface/volume ratio compared to bulk materials [62–69]. Nanoflowers, on the other hand, are frequently created under extreme circumstances, such as high temperatures, pressure, and the use of dangerous chemical solvents. As a result, developing a low-cost, straightforward synthetic approach for producing hierarchical nanoflowers remains a challenge. Consequently, self-assembled pattern synthesis provides a simple and efficient low-temperature synthetic method for

producing well-defined nanoflowers. Bioinspired materials with microscale and nanoscale have been highlighted as a key development in the design of functional materials [70–72] due to the tremendous leadership of biomolecules in guiding and creating nanoflowers. Biomolecules such as enzymes [73–78], proteins [79], and amino acids [80] were used to make nanoflower. For the first time, Zare's group outlined the creation of hybrid nanoflowers made of $Cu_3(PO_4)_2$ and proteins, as well as the production of immobilized enzymes with significantly improved activity [81]. Wang et al. (2013) then used the same synthesis procedure to make $CaHPO_4$-*a*-amylase nanoflowers, as well as clarifying the mechanism underlying the immobilized enzyme's improved catalytic activity [82]. Though biodegradable amphiphilic molecules have been widely used throughout nanomaterial manufacturing, the self-assembly process facilitated by amphiphilic molecules can provide a potent low-temperature tool for the creation of hierarchical structures, bio-surfactants have not been widely reported in the fabrication of nanoflowers [83,84].

Using copper (II) ions as the inorganic component and different extracts from *Aspergillus terreus* and its isolated major components as the organic component, this study describes a simple and successful self-assembled template synthesis technique for three-dimensional (3D) flower-like $Cu_3(PO_4)_2$ nanostructures. The hybrid nanoflowers were characterized using scanning electron microscopy (SEM), Fourier transform infrared spectroscopy (FT-IR), energy-dispersive X-ray spectroscopy (EDX), and X-ray diffraction (XRD). For some bacteria, the produced hybrid nanoflowers showed exceptional antibacterial activity.

2. Material and Methods

2.1. Materials and Reagents

2.1.1. Fungal Material

A. terreus fungus was isolated from the *Spirorbis* sp., which was obtained by biolog Bülent Gözcelioğlu from Marmara Sea in 2018. For identification, this fungus was cultured on Sabouraud 4% dextrose agar (SDA, Merck, Germany) at room temperature for a week in an incubator (Nüve, Turkey). The fungus was identified as *Aspergillus terreus* (GenBank accession number MT273950) based on DNA amplification and ITS (internal transcribed spacer) sequencing data analysis [85].

2.1.2. Chemical Material and Reagents

All chemicals were provided by Sigma-Aldrich Products, St. Louis, MO, USA. Chromatographic separation procedures were performed by applying column chromatography with stationary phases as silica gel 60 M (0.04–0.063 mm). For screening purposes, ready-made silica gel 60 F_{254} Thin Layer Chromatography (TLC) plates (Merck, Darmstadt, Germany) were used. Ethyl acetate (EtOAc) Ph. Eur., BP, NF with >99.5% purity, Petroleum Ether boiling range 40–60 °C, with >75.0% purity, Dichloromethane (DCM) Ph. Eur., NF with >99.0% purity was used for fermentation and secondary metabolite isolation processes.

2.1.3. Extraction of *Aspergillus Terreus*

Solid rice medium was prepared and sterilized by autoclave for cultivation of fungal strain. Pieces of fungus in Petri dishes were transferred to Erlenmeyer flasks containing the medium. Fermentation process continued for 4 weeks at room temperature in dark and under static conditions.

To end fermentation process, 350 mL (EtOAc) was added to each flask. Flasks were placed in orbital shaker for 12 h before filtering, and EtOAc filtrate was gathered and vaporized under optimized vaccuum until obtaining crude extract (16.41 g). Separation of crude extract by liquid–liquid extraction and fractionation process was completed according to the previous methodology [85].

2.1.4. Isolation of Butyrolactone I and Butyrolactone III

Obtained fractions from fungi extract were applied to chromatographic methods. Second fraction (DCM 100%) was determined to apply more chromatographic processes to isolate and purify compounds. Second fraction (3072 mg) was subjected to column loaded with silica gel as column packing material and petroleum ether:EtOAc as mobile phase at ratios of 4:1, 3:1, 2:1, and 1:1, each 300 mL, respectively, yielding Butyrolactone I and Butyrolactone III. Portions of 10 mL eluates were checked with TLC and merged to obtain compounds.

Butyrolactone I was obtained as an amorphous solid with orange color. Ultraviolet (UV) spectra of compound demonstrated 2 absorption maxima (λ_{max}) at 307 and 210 nm. From the information obtained from Mass Spectrometry (MS), the molecular formula was decided to be $C_{24}H_{24}O_7$. Nuclear Magnetic Resonance (NMR) data of compound were compared with the fungal metabolites recorded in the literature; it was revealed that there was an agreement with butyrolactone I [85].

Butyrolactone III was obtained as a yellow amorphous solid with λ_{max} in UV spectra at 308 and 225 nm. The MS of compound presented 2 pseudo molecular ion peaks at *m*/*z* 463.12586 [M + Na]+ (calcd for $C_{24}H_{24}O_8Na$, 463.13091) and at *m*/*z* 439.11538 [M-H]- (calcd for $C_{24}H_{23}O_8$, 423.12212) remarking the compound to be $C_{24}H_{24}O_8$. Checking the NMR spectra of compound with known compounds, compound was defined as butyrolactone III [86,87].

2.2. Instrumentation

2.2.1. General Experimental Procedures

The fungi isolation was carried out in a laminar flow cabin (Holten, USA). Buchi R-300 (Switzerland) rotary evaporator systems were used for evaporating solvents and obtaining dry crude fungi extract.

Chromatographic separation procedures were performed according to the previous methodology [82]. Last purification of isolated compounds was completed by Agilent 1100 Series HPLC system and structures of compounds elucidated with help of a Bruker Avance 400 MHz spectrometer (Massachusetts, USA) were used for 1D (^{1}H and ^{13}C NMR) and 2D NMR spectra (chemical shifts in ppm) and Agilent 6230B Time of Flight (TOF) LC/MS (Santa Clara, CA, USA) data.

2.2.2. Synthesis of Hybrid Nanoflowers and Characterization

A total of 1 mL *A. terreus* extract and its purified components (1 mg/mL) were added separately to 50 mL phosphate-buffered saline (PBS) solution (50 mM, pH 7) and 20 mL $CuSO_4$ solution (120 mM). The combination was then incubated for 3 days at 25 degrees Celsius. At the bottom of the flash, there appeared a blue precipitate. Finally, the blue color precipitate was centrifuged (12,000 rpm for 20 min) to remove the solution's supernatant and rinsed 3 times with deionized water for further analysis. The morphology of the synthesized hybrid nanoflowers was examined using SEM, EDX, XRD, and FT-IR. A scanning electron microscope (SEM) is a type of electron microscope that produces images by scanning the sample surface with a concentrated stream of electrons. Electrons interact with atoms in the sample to provide a variety of signals, including information about the topography and composition of the sample surface. These signals are captured by the requisite detectors, which are subsequently transferred to the computer screen, where a picture is generated. The EDX system performs a point, line, area scan, and X-ray mapping of a given area, and elemental analyses can be conducted in these regions, both qualitatively and quantitatively. The X-Ray Diffraction (XRD) approach is based on the idea that each crystal phase refracts X-rays in a distinct manner depending on its atomic arrangement. These diffraction profiles for each crystal phase serve as a fingerprint for that crystal. FTIR stands for Fourier Transform Infrared Spectroscopy and is used to identify organic, polymeric, and, in certain cases, inorganic materials. The FTIR analysis technique uses infrared light to scan test samples and determine chemical properties. The chemical

fingerprint of the sample is represented by the resulting signal at the detector, which appears as a spectrum ranging from 4000 cm^{-1} to 400 cm^{-1}. Each molecule or chemical structure has a unique spectral fingerprint.

In the rest of this text, *Aspergillus*-Nanoflowers, Butyrolactone I-Nanoflowers, and Butyrolactone III-Nanoflowers were abbreviated as (A-NFs), (B(I)-NFs), and (B(III)-NFs), respectively.

2.3. Antimicrobial Activity

2.3.1. Bacterial Strains and Growth Conditions

The standard strains were obtained from the ATCC, VA, USA: *Aeromonas hydrophila* (ATCC 7966), *Aeromonas sobria* (ATCC 43979), *Escherichia coli* (ATCC 25922), *Salmonella enterica* (ATCC 13076), and *Staphylococcus aureus* (ATCC 25923). The antibacterial activity of *A. terreus* extracts and its isolated major components was detected against the selected bacteria. Pure cultures of bacteria were sub-cultured on Mueller Hinton Agar (MHA) at 37 °C for 24 h, and each bacterium was then suspended according to 0.5 McFarland [16]. All the antibacterial susceptibility assays were performed in triplicate.

2.3.2. Disk Diffusion Method

Disk diffusion tests were carried out according to the method of Bauer et al. (1966) [88]. Each bacterial suspension, previously diluted to 0.5 McFarland turbidity standards, was evenly spread on a solid MHA in a Petri dish using sterile cotton swab. Sterile paper discs with a diameter of 6 mm were impregnated with 20 µL of extract, and these discs were placed on the surface of the agar plate. Empty disks were used as a negative control. The plates were incubated at 37 °C for 24 h, and then the diameter of inhibition zone was measured using a ruler.

2.3.3. Minimum Inhibitory Concentration (MIC)

The MIC of extracts was determined using broth microdilution method. Different concentrations (0.25, 0.5, 1, 2, 4, 8, 16, 32, 64, 128, 256, 512, and 1024 µg/mL) of extracts were diluted with 100 µL of Mueller–Hinton broth by 2-fold serial dilution. Then, 10 µL of the tested bacteria previously diluted to 0.5 McFarland turbidity standard was added into each microtiter plate. Microtiter plates inoculated bacterial cultures were then incubated at 37 °C for 24 h. Therefore, negative (only medium) and positive (medium and bacterial inoculums) controls were performed [89].

3. Results

3.1. Synthesis and Characterization of Organic–Inorganic Hybrid Nanoflowers

To make the flower-like structures in our study, we first used the *A. terreus* extract and its isolated main components as an organic component. The mechanism for creating organic–inorganic hybrid nanoflowers has previously been disclosed [38,40,41,44,45,90].

The nanoflowers (NFs) were formed in three stages: nucleation, growth, and conclusion of formation. (1) Primary copper phosphate nanocomplexes were formed from Cu2+ and phosphate ions in the nucleation step, and they primarily bound to amide groups and/or carboxyl and diol groups of organic components to form seeds; (2) primary nanocrystals continued to react with organic molecules in the growth step, and petal-like structures appeared; and (3) NFs were completely formed by sticking petals in the final step [73,81,90–97].

When the amide and diol groups of molecules connect with the copper phosphate complex, A-NFs-Cu^{2+}, B(I)-NFs-Cu^{2+}, and B(III)-NFs-Cu^{2+} are generated. To validate our design, Cu^{2+} ions and fungal extract were mixed in the PBS solution, and blue precipitates were generated after 3 days of incubation (Figure 1).

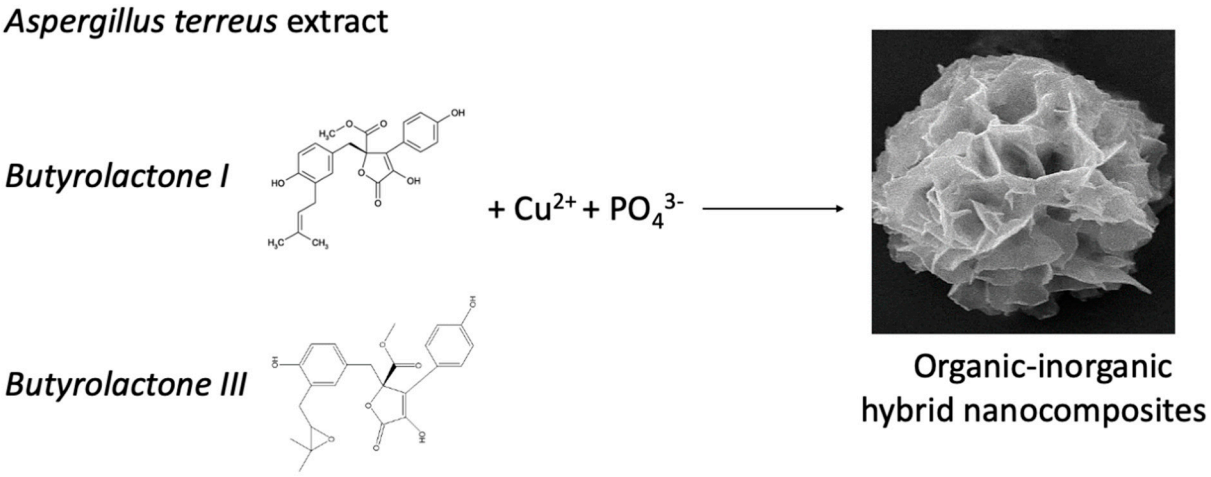

Figure 1. Schematic illustration of amide and diol groups of molecules extracted from *A. terreus* bind with the copper phosphate complex.

According to research by Mutti et al. and Łyskowski et al., the (R)-ω-transaminase from *Aspergillus terreus* (AT-ωTA) has been demonstrated to preferentially convert aliphatic substrates (chain length up to at least six carbons) with a high yield and high enantioselectivity [98,99].

The A-NFs, B(I)-NFs, and B(III)-NFs had spherical morphologies with narrow size distributions between 11–16 µm, as observed in the SEM images for A-NFs (~11–16 µm), B(I)-NFs (~12–15 µm), and B(III)-NFs (~13–14 µm) in Figure 2. The structure of the hybrid nanoflowers (hNFs) was verified using EDX, XRD, and FTIR. To identify functional groups, FTIR was performed to investigate the chemical structures of free extract and the Cu^{2+} hNFs extract. The *A. terreus* extract, Butyrolactone I, Butyrolactone III, and A-NFs, B(I)-NFs, B(III)-NFs -Cu^{2+} powder were dried at 60 °C prior to FTIR sample preparation. Simply put, each powder was mixed separately with IR grade K Br before being crushed into tablets. The distinctive peaks of the free extract of *A. terreus*, Butyrolactone I, and Butyrolactone III in Figure 3, and A-NFs, B(I)-NFs, B(III)-NFs -Cu^{2+} in Figure 4 were studied on the FTIR spectra. At ~985 cm^{-1}, the O-P-O (the (oxygen-phospate-oxygen) bond between the phosphate atom and oxygen atoms in PO_4) groups showed lesser bending vibration. However, at ~987 cm^{-1}, the same vibration manifested in a very strong form. The vibration bands of the NH_2 groups of the *A. terreus,* Butyrolactone I, and Butyrolactone III extracts, and A-NFs, B(I)-NFs, B(III)-NFs-Cu^{2+} hNFs appeared at ~1646 cm^{-1} and ~1729 cm^{-1}, ~1732 cm^{-1}, 1623 cm^{-1}, 1622 cm^{-1}, and 1622 cm^{-1}, respectively. Finally, the CH_3 and CH_2 groups of the *A. terreus* extract, Butyrolactone I, Butyrolactone III, and A-NFs, B(I)-NFs, B(III)-NFs -Cu^{2+} were assigned to its stretching bands at 2800–3429 cm^{-1}. The crystalline structures of the nanoflowers and $Cu_3(PO_4)H_2O$ were revealed by the XRD patterns in Figure 5. The findings showed that all of the diffraction peaks in Figure 5 well matched the JCPDS card (00–022–0548) in terms of their locations and relative intensities, demonstrating that the hybrid nanoflowers had high crystallinity and were well crystallized. These results demonstrated that Cu NFs were successfully produced by reacting several *Aspergillus terreus* extracts with their recovered primary components and Cu ions in PBS buffer. The EDX spectrum and mapping of *Aspergillus terreus* extract, Butyrolactone I, Butyrolactone III, and organic–inorganic NFs showed the presence of Cu and other components in the structure of the hNFs. The weight % of Cu in the hNFs was found to be 20.7%, 20.2%, and 8.9% using *Aspergillus terreus* extract, Butyrolactone I, and Butyrolactone III, respectively. Additionally, EDX mapping was used to confirm the distribution of the four essential elements in the hNFs, which are C (blue), O (turquoise), P (red), N (green), and Cu (yellow) (Figure 6).

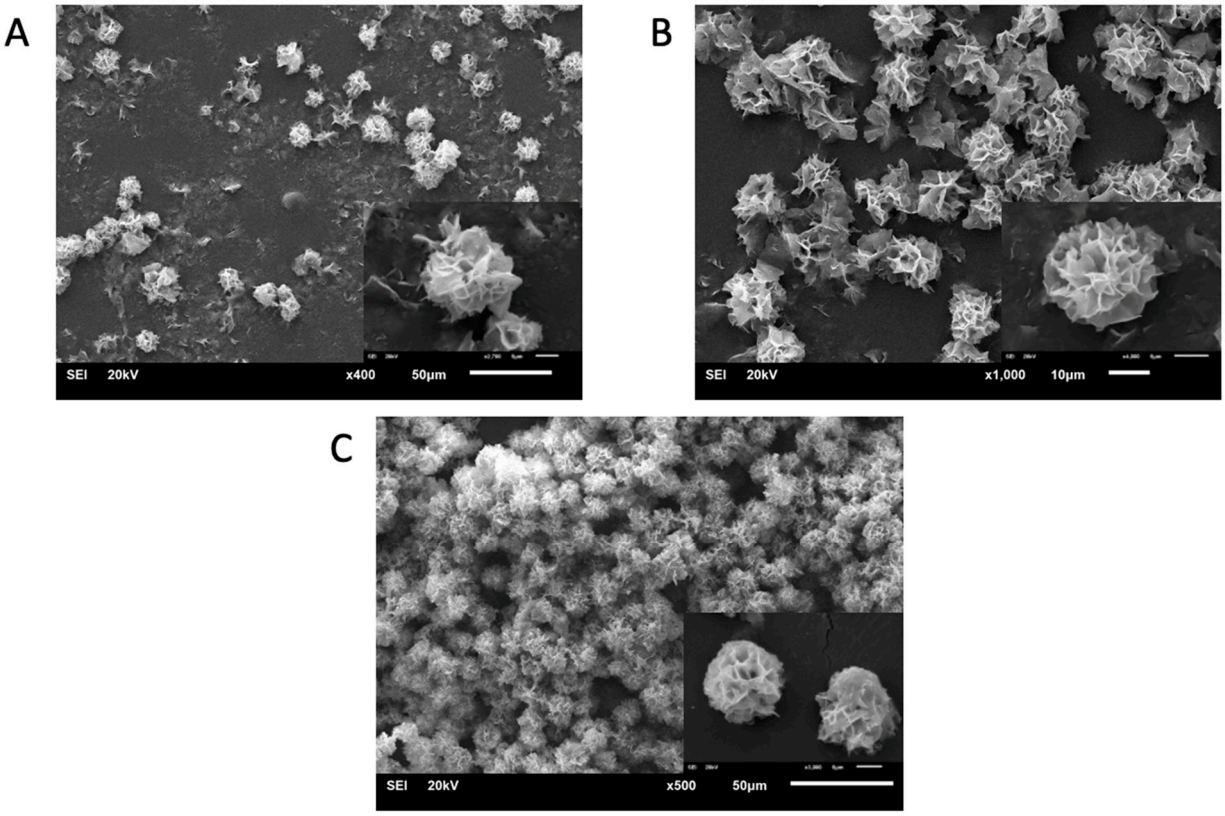

Figure 2. SEM images of (**A**) *Aspergillus terreus* extract (~11–16 µm), (**B**) Butyrolactone I (~12–15 µm), and (**C**) Butyrolactone III (~13–14 µm) organic–inorganic NFs.

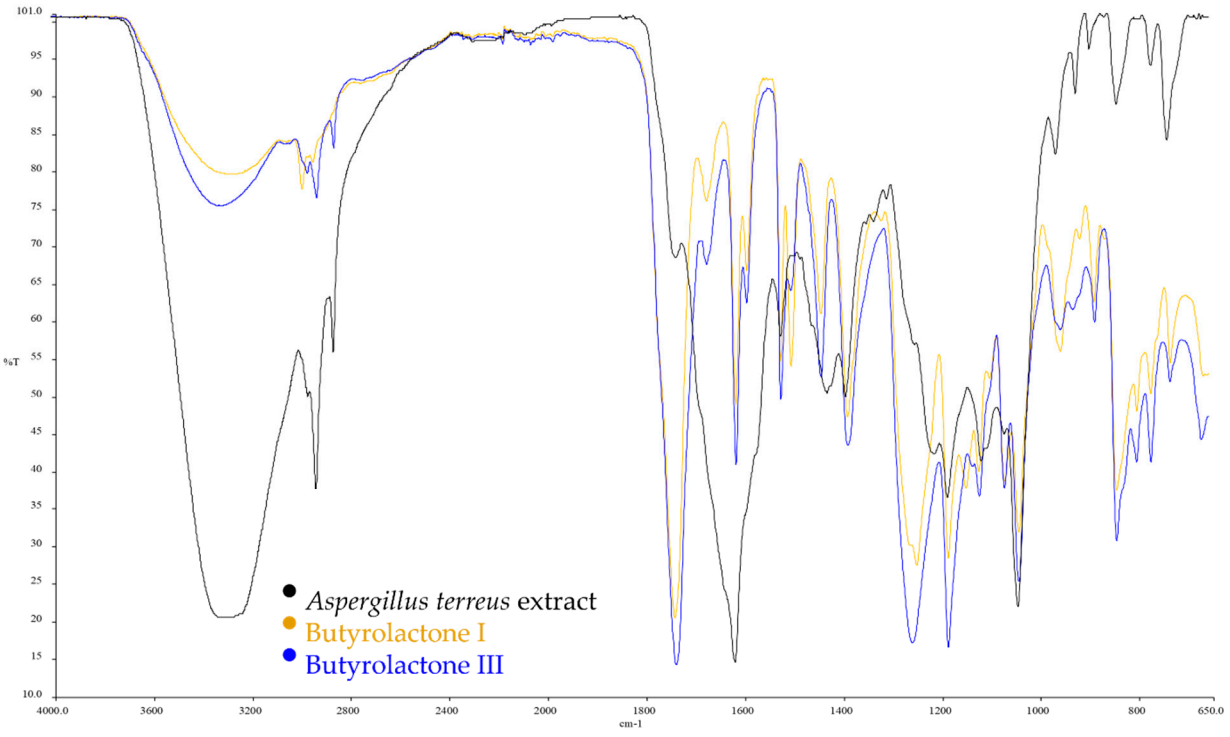

Figure 3. FTIR of *Aspergillus terreus* extract, Butyrolactone I, and Butyrolactone III.

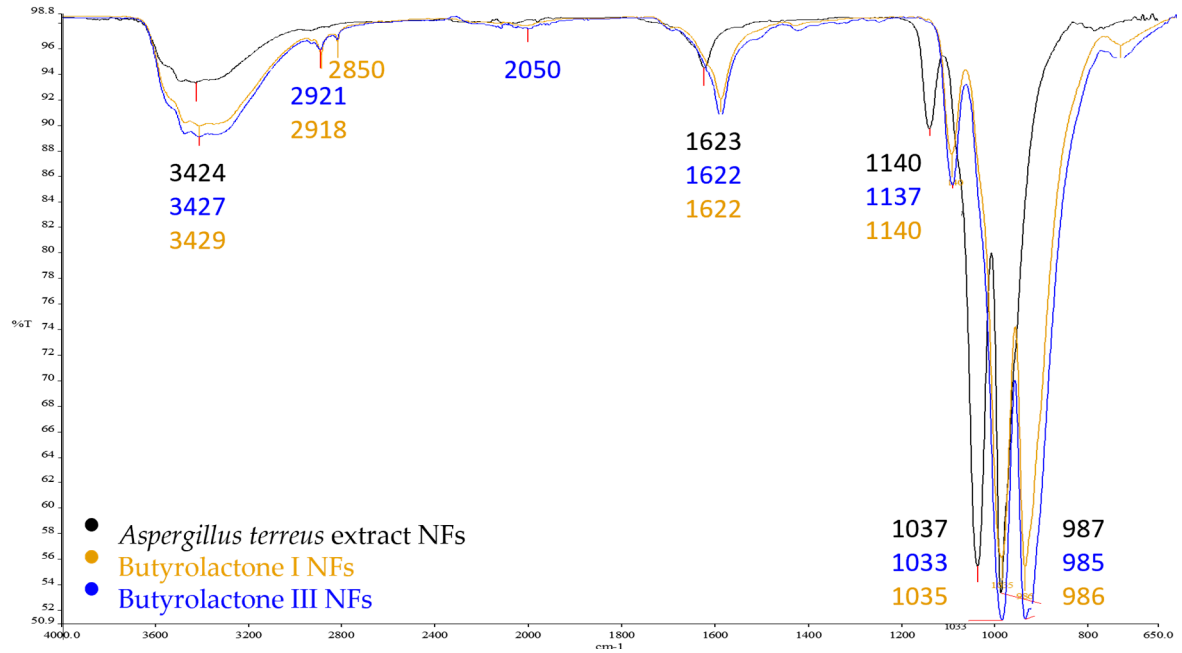

Figure 4. FTIR of *Aspergillus terreus* extract, Butyrolactone I, and Butyrolactone III organic–inorganic NFs.

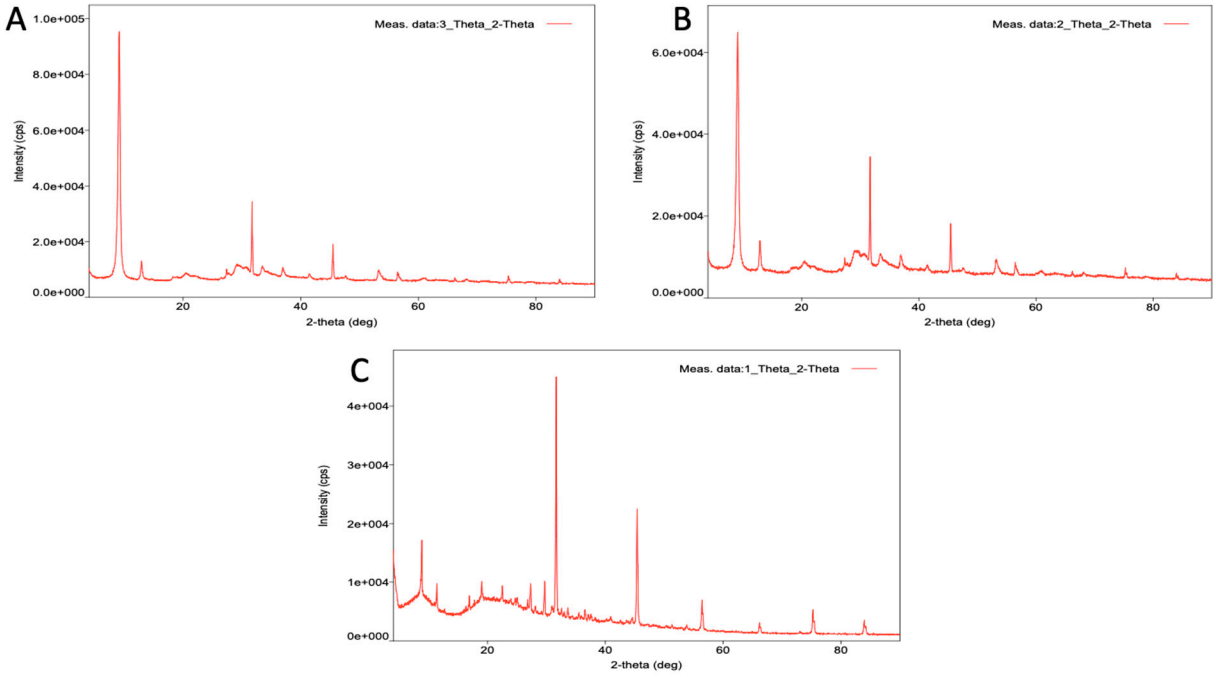

Figure 5. XRD of (**A**) *Aspergillus terreus* extract, (**B**) Butyrolactone I, and (**C**) Butyrolactone III organic–inorganic NFs.

3.2. Analysis of Antimicrobial Activity

The A-NFs, B(I)-NFs, and B(III)-NFs had greater antibacterial activity against all tested pathogen bacteria compared to their extract groups, and the data of all nanoflower groups were statistically similar ($p < 0.05$). Butyrolactone III only had an inhibition zone on *A. hydrophila*, while Butyrolactone I had an inhibition zone on *A. hydrophila* and *E. coli*. However, *A. terreus* did not show antibacterial activity against any bacteria tested, and no inhibition zone was seen (Figure 7). According to the results, *A. hydrophila* and *S. aureus* were more sensitive to the extracts than other bacteria.

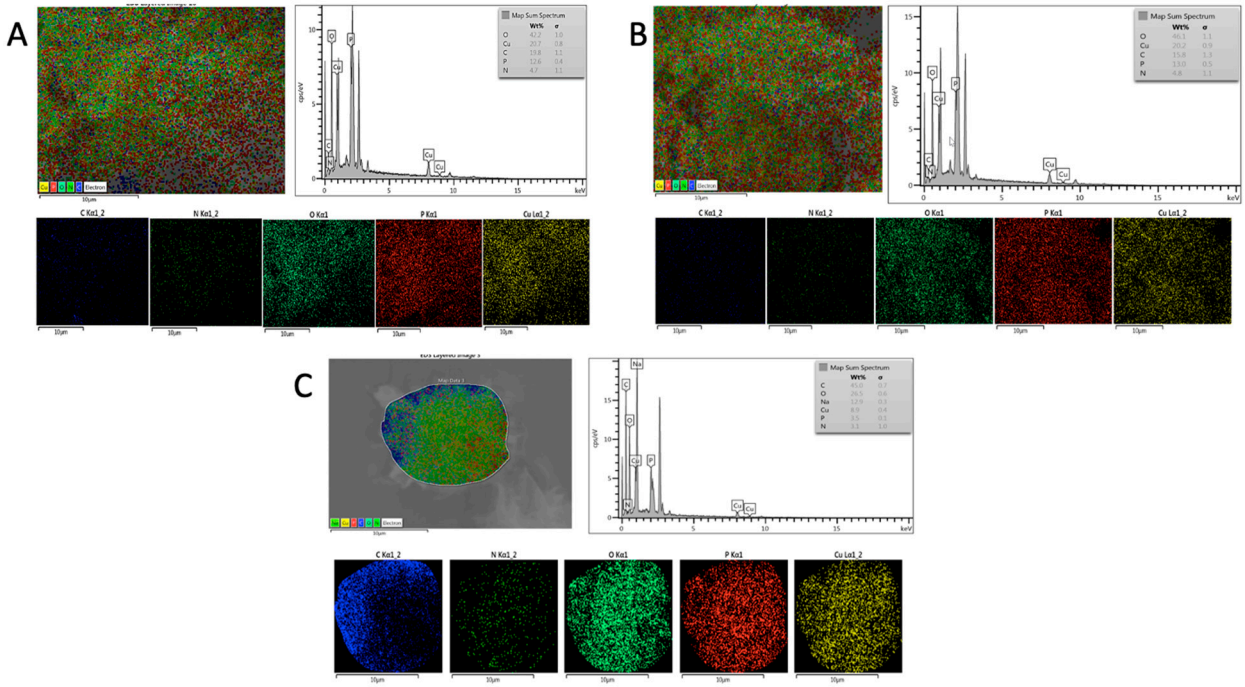

Figure 6. Using EDX Mapping to examine and show the components of C, O, P, N, and Cu with various colors of (**A**) *Aspergillus terreus* extract, (**B**) Butyrolactone I, and (**C**) Butyrolactone III, hNFs.

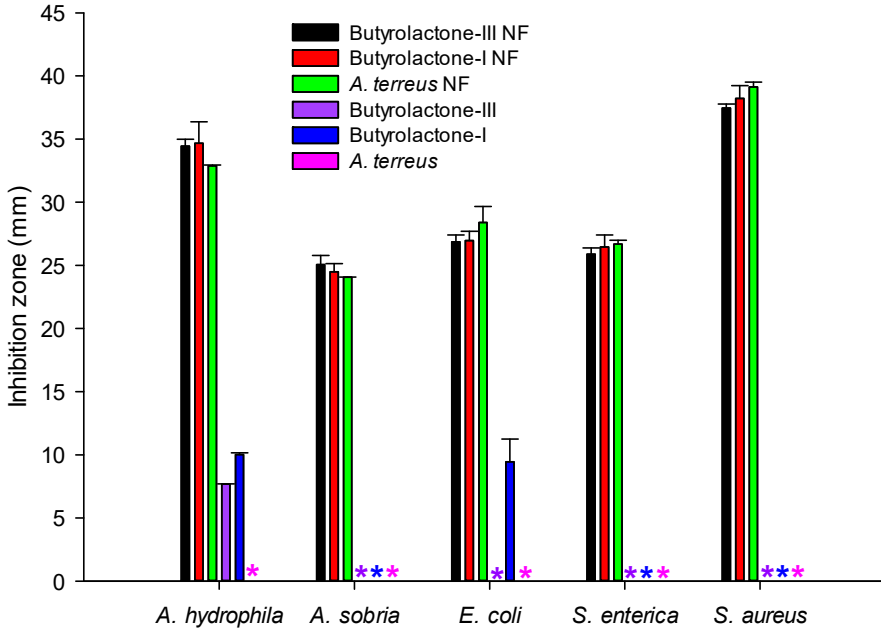

Figure 7. Antibacterial activity of the *A. terreus* and Butyrolactone extracts against tested pathogen bacteria. *: No inhibition zone. NF: Nanoflower.

The MICs of extracts varied against different tested strains: A-NFs and B(III)-NFs against *A. hydrophila*, A-NFs against *A. sobria*, B(III)-NFs against *E. coli*, and B(I)-NFs and A-NFs against *S. enterica*. All nanoflower groups against *S. aureus* were determined to have the most effective antibacterial effect according to the MIC analysis (Table 1). All extracts with a nanoflower showed antibacterial activity against all bacteria tested. Similar to the results of the disc diffusion method: nanoflower groups had more antibacterial activity compared to other extracts. However, some of the non-nanoflower extracts did not show any antibacterial effect against all bacteria tested, and all bacteria grew on all microtiter

plates of these extracts. According to MIC results, *A. hydrophila* was more sensitive to the extracts than other pathogen bacteria tested. Based on the antimicrobial results obtained in this present study, it was determined that nanoflower treatment provided significant antimicrobial properties to the extracts of *A. terreus* and Butyrolactone.

Table 1. Minimum inhibitory concentration (μg/mL) of the extracts against tested pathogen bacteria.

Extracts	*A. hydrophila*	*A. sobria*	*E. coli*	*S. enterica*	*S. aureus*
B(III)-NFs	8	64	32	64	16
B(I)-NFs	16	64	64	32	16
A-NFs	8	32	64	32	16
Butyrolactone III	1024	+	+	+	1024
Butyrolactone I	512	1024	1024	1024	1024
A. terreus	+	1024	+	+	+

+: Growth in all concentrations. NF: Nanoflower.

Over the last few decades, many studies have been carried out on the investigation of antimicrobial activities as well as antioxidant properties of various plants and their compounds. In addition, the interest of researchers has increased rapidly because they have alternative potentials in terms of being both non-toxic and cheaper compared to synthetic materials. Li et al. (2012) reported that the AgNPs produced by *A. terreus* exhibited antibacterial activity in *S. aureus*, *P. aeruginosa,* and *E. coli* with 16 mm, 12 mm, and 13 mm inhibition zone, respectively [100]. Bunbamrung et al. (2020) reported 7 of 31 compounds isolated from marine-derived *A. terreus* exhibited antibacterial activity against *B. cereus* with MIC values in the range of 12.5–50.0 mg/mL [101]. Jain and Pundir (2010) investigated the effect of different carbon and nitrogen sources on the antimicrobial metabolite of *A. terreus*, and they reported that dextrose as a carbon source (22 to 26 mm) and sodium nitrate (20 to 28 mm) as nitrogen source may be used for maximum production of the antimicrobial metabolite from *A. terreus* according to agar well-diffusion assay [102]. In this present study, nanoflower compounds from *A. terreus* against the bacteria tested reached a higher inhibition zone (25.06 to 38.22 mm) than those reported by Jain and Pundir (2010) [102]. On the other hand, the results of Jain and Pundir (2010) were similar to our data in that the antimicrobial metabolite of *A. terreus* against *S. aureus* (max. 26 mm) was higher than *E. coli* (max. 24 mm). San-Martin et al. (2011) investigated the antibacterial activity of Butyrolactone I and Butyrolactone VI isolated from *Aspergillus* sp. against *Pseudomonas syringae* pv syringae, *Xanthomonas arboricola* pv juglandis 833, *Erwinia carotovora*, *Agrobacterium tumefaciens* A348, and *Clavibacter michiganensis* 807 [103]. They reported that these compounds showed antibacterial activity only against *C. michiganensis*. In another study, Cazar et al. (2005) reported that Butyrolactone I isolated from soil fungus *A. terreus* had stronger inhibitory effect against *Erwinia carotovora,* and it had antibacterial activity against *Bacillus subtilis* and *Enterobacter dissolvens.* However, they did not determine any antibacterial activity of Butyrolactone III against all bacteria tested [14]. Similarly, we determined that Butyrolactone I had higher inhibitory activity than Butyrolactone III. Orfali et al. (2021) reported that the antibacterial activity of Butyrolactone derivatives isolated from the marine-derived genus *Aspergillus* has the highest rate of 25% compared to the distribution of other metabolites [7]. These results indicated that nanoflowers of antibacterial compounds produced from the marine fungi *A. terreus* might be used for medicines in the future. Many methods are used to determine the antimicrobial activities of extracts. However, as these methods are not all based on the same principles, the results determined are affected not only by the method chosen but also by the extraction method used and the microorganism species or solubility degree of the test compound [104]. Accordingly, the differences obtained from both previous studies and the present study data can be attributed to these factors.

4. Conclusions

Finally, isolated secondary metabolites and the extract from *Aspergillus terreus*-assisted self-assembly with copper ions were employed to create simple and successful 3D nanostructures. The resulting hybrid nanoflowers have a flower-like hierarchical structure, a huge surface area, and increased antibacterial action. Furthermore, no morphological deformation was seen under SEM, showing that the nanoflowers are mechanically stable.

Marine-derived *Aspergillus terreus* produces a variety of structurally important secondary metabolites, the majority of which have unique biological features that can be used in medicine. In addition, microbial sources are increasingly being used to produce nanoparticles for cancer therapy. A-NFs, B(I)-NFs, and B(III)-NFs have prospective benefits in human health as a therapeutic agent to overcome rising antibiotic resistance against harmful microbes due to their ability to overcome drug resistance.

Author Contributions: B.K. (Belma Konuklugil) and I.O. conceptualized and designed the study. I.S.U. and B.K. (Baris Karsli) conducted experiments. B.K. (Belma Konuklugil) and A.D. analyzed data. A.D. wrote the manuscript. All authors have read and agreed to the published version of the manuscript.

Funding: The Turkish Scientific and Technological Research Council (TUBITAK) funded this research (grant number 114S916). The funder was not involved in the study design, data collection and analysis, publication decision, or manuscript writing.

Institutional Review Board Statement: Not applicable.

Informed Consent Statement: Not applicable.

Data Availability Statement: The datasets generated during and/or analyzed during the current study are available from the corresponding author upon reasonable request.

Acknowledgments: Bülent Gözcelioğlu, who collected marine organisms for the study, is acknowledged by the authors.

Conflicts of Interest: The authors declare no conflict of interest.

References

1. Khalifa, S.A.M.; Elias, N.; Farag, M.A.; Chen, L.; Saeed, A.; Hegazy, M.F.; Moustafa, M.S.; Abd El-Wahed, A.; Al-Mousawi, S.M.; Musharraf, S.G.; et al. Marine natural products: A source of novel anticancer drugs. *Mar. Drugs* **2019**, *17*, 491. [CrossRef] [PubMed]
2. Wang, C.; Tang, S.; Cao, S. Antimicrobial compounds from marine fungi. *Phytochem. Rev.* **2021**, *20*, 85–117. [CrossRef]
3. Kamat, S.; Kumar, S.; Philip, S.; Kumari, M. Secondary Metabolites from Marine Fungi: Current Status and Application. In *Microbial Biomolecules*; Kumar, A., Bilal, M., Ferreira, L.F.R., Kumari, M., Eds.; Academic Press: Cambridge, MA, USA, 2023; pp. 181–209.
4. Javed, F.; Qadir, M.I.; Janbaz, K.H.; Ali, M. Novel drugs from marine microorganisms. *Crit. Rev. Microbiol.* **2011**, *37*, 245–249. [CrossRef]
5. Blunt, J.W.; Copp, B.R.; Hu, W.-P.; Munro, M.H.G.; Northcote, P.T.; Prinsep, M.R. Marine natural products. *Nat. Prod. Rep.* **2009**, *26*, 170–244. [CrossRef]
6. Bugni, T.S.; Ireland, C.M. Marine-derived fungi: A chemically and biologically diverse group of microorganisms. *Nat. Prod. Rep.* **2004**, *21*, 143–163. [CrossRef] [PubMed]
7. Orfali, R.; Aboseada, M.A.; Abdel-Wahab, N.M.; Hassan, H.M.; Perveen, S.; Ameen, F.; Alturki, E.; Abdelmohsen, U.R. Recent updates on the bioactive compounds of the marine-derived genus *Aspergillus*. *RSC Adv.* **2021**, *11*, 17116–17150. [CrossRef]
8. Luo, X.-W.; Lin, Y.; Lu, Y.-J.; Zhou, X.F.; Liu, Y.H. Peptides and polyketides isolated from the marine sponge-derived fungus *Aspergillus terreus* SCSIO 41008. *Chin. J. Nat. Med.* **2019**, *17*, 149–154. [CrossRef] [PubMed]
9. Chen, M.; Wang, K.-L.; Liu, M.; She, Z.-G.; Wang, C.-Y. Bioactive Steroid Derivatives and Butyrolactone Derivatives from a Gorgonian-Derived *Aspergillus* sp. Fungus. *Chem. Biodivers.* **2015**, *12*, 1398–1406. [CrossRef] [PubMed]
10. Sun, Y.; Liu, J.; Li, L.; Gong, C.; Wang, S.; Yang, F.; Hua, H.; Lin, H. New butenolide derivatives from the marine sponge-derived fungus Aspergillus terreus. *Bioorganic Med. Chem. Lett.* **2018**, *28*, 315–318. [CrossRef]
11. Zeng, Q.; Zhong, W.-M.; Chen, Y.-C.; Xiang, Y.; Chen, X.-Y.; Tian, X.-P.; Zhang, W.-M.; Zhang, S.; Wang, F.-Z. A new butenolide derivative from the deep-sea fungus *Aspergillus terreus* SCSIO FZQ028. *Nat. Prod. Res.* **2020**, *34*, 1984–1991. [CrossRef] [PubMed]
12. Malik, P.; Shankar, R.; Malik, V.; Sharma, N.K.; Mukherjee, T.K. Green Chemistry Based Benign Routes for Nanoparticle Synthesis. *J. Nanoparticles* **2014**, *2014*, 302429. [CrossRef]

13. Patra, D.; El Kurdi, R. Curcumin as a novel reducing and stabilizing agent for the green synthesis of metallic nanoparticles. *Green Chem. Lett. Rev.* **2021**, *14*, 474–487. [CrossRef]
14. Cazar, M.-E.; Schmeda-Hirschmann, G.; Astudillo, L. Antimicrobial Butyrolactone I Derivatives from the Ecuadorian Soil Fungus Aspergillus terreus Thorn. var terreus. *World J. Microbiol. Biotechnol.* **2005**, *21*, 1067–1075. [CrossRef]
15. Rani, R.; Sharma, D.; Chaturvedi, M.; Yadav, J.P. Green Synthesis, Characterization and Antibacterial Activity of Silver Nanoparticles of Endophytic Fungi *Aspergillus terreus*. *J. Nanomed. Nanotechnol.* **2017**, *8*, 1000457. [CrossRef]
16. Karslı, B. Antibacterial and antioxidant activity of pulp, peel and leaves of Feijoa sellowiana: Effect of extraction techniques, solvents and concentration. *Food Health* **2021**, *7*, 21–30. [CrossRef]
17. Oladipo, A.O.; Nkambule, T.T.I.; Mamba, B.B.; Msagati, T.A.M. Therapeutic nanodendrites: Current applications and prospects. *Nanoscale Adv.* **2020**, *2*, 5152–5165. [CrossRef]
18. Oladipo, A.O.; Unuofin, J.O.; Iku, S.I.; Nkambule, T.T.; Mamba, B.B.; Msagati, T.A. Bimetallic Au@Pd nanodendrite system incorporating multimodal intracellular imaging for improved doxorubicin antitumor efficiency. *Int. J. Pharm.* **2021**, *602*, 120661. [CrossRef]
19. Oladipo, A.O.; Unuofin, J.O.; Iku, S.I.; Nkambule, T.T.; Mamba, B.B.; Msagati, T.A. Nuclear targeted multimodal 3D-bimetallic Au@Pd nanodendrites promote doxorubicin efficiency in breast cancer therapy. *Arab. J. Chem.* **2021**, *14*, 103344. [CrossRef]
20. Leena, M.M.; Anukiruthika, T.; Moses, J.; Anandharamakrishnan, C. Co-delivery of curcumin and resveratrol through electrosprayed core-shell nanoparticles in 3D printed hydrogel. *Food Hydrocoll.* **2021**, *124*, 107200. [CrossRef]
21. Nguyen, T.T.; Van Dao, D.; Ha, N.T.T.; Van Tran, T.; Kim, D.-S.; Yoon, J.-W.; Lee, I.-H.; Yu, Y.-T. Superhigh sensing response and selectivity for hydrogen gas using PdPt@ZnO core-shell nanoparticles: Unique effect of alloyed ingredient from experimental and theoretical investigations. *Sens. Actuators B Chem.* **2022**, *354*, 131083. [CrossRef]
22. Pajor-Świerzy, A.; Szczepanowicz, K.; Kamyshny, A.; Magdassi, S. Metallic core-shell nanoparticles for conductive coatings and printing. *Adv. Colloid Interface Sci.* **2022**, *299*, 102578. [CrossRef] [PubMed]
23. Kim, K.; Chae, S.; Choi, P.G.; Itoh, T.; Saito, N.; Masuda, Y. Facile synthesis of ZnO nanobullets by solution plasma without chemical additives. *RSC Adv.* **2021**, *11*, 26785–26790. [CrossRef]
24. Thangavelu, R.M.; Gunasekaran, D.; Jesse, M.I.; SU, M.R.; Sundarajan, D.; Krishnan, K. Nanobiotechnology approach using plant rooting hormone synthesized silver nanoparticle as "nanobullets" for the dynamic applications in horticulture—An in vitro and ex vitro study. *Arab. J. Chem.* **2018**, *11*, 48–61. [CrossRef]
25. Wang, Z.; Zhang, F.; Shao, D.; Chang, Z.; Wang, L.; Hu, H.; Zheng, X.; Li, X.; Chen, F.; Tu, Z.; et al. Janus Nanobullets Combine Photodynamic Therapy and Magnetic Hyperthermia to Potentiate Synergetic Anti-Metastatic Immunotherapy. *Adv. Sci.* **2019**, *6*, 1901690. [CrossRef]
26. Hoang, A.T.; Nižetić, S.; Cheng, C.K.; Luque, R.; Thomas, S.; Banh, T.L.; Pham, V.V.; Nguyen, X.P. Heavy metal removal by biomass-derived carbon nanotubes as a greener environmental remediation: A comprehensive review. *Chemosphere* **2022**, *287*, 131959. [CrossRef] [PubMed]
27. Ibusuki, R.; Morishita, T.; Furuta, A.; Nakayama, S.; Yoshio, M.; Kojima, H.; Oiwa, K.; Furuta, K. Programmable molecular transport achieved by engineering protein motors to move on DNA nanotubes. *Science* **2022**, *375*, 1159–1164. [CrossRef]
28. Saha, T.; Dash, C.; Jayabalan, R.; Khiste, S.; Kulkarni, A.; Kurmi, K.; Mondal, J.; Majumder, P.K.; Bardia, A.; Jang, H.L.; et al. Intercellular nanotubes mediate mitochondrial trafficking between cancer and immune cells. *Nat. Nanotechnol.* **2022**, *17*, 98–106. [CrossRef]
29. Sawant, S.V.; Patwardhan, A.W.; Joshi, J.B.; Dasgupta, K. Boron doped carbon nanotubes: Synthesis, characterization and emerging applications—A review. *Chem. Eng. J.* **2022**, *427*, 131616. [CrossRef]
30. Arjmand, T.; Legallais, M.; Nguyen, T.T.T.; Serre, P.; Vallejo-Perez, M.; Morisot, F.; Salem, B.; Ternon, C. Functional Devices from Bottom-Up Silicon Nanowires: A Review. *Nanomaterials* **2022**, *12*, 1043. [CrossRef]
31. Clarke, T.A. Plugging into bacterial nanowires: A comparison of model electrogenic organisms. *Curr. Opin. Microbiol.* **2022**, *66*, 56–62. [CrossRef] [PubMed]
32. Lee, H.Y.; Kim, S. Nanowires for 2D material-based photonic and optoelectronic devices. *Nanophotonics.* **2022**, *11*, 2571–2582. [CrossRef]
33. Yang, Z.; Pan, X.; Shen, Y.; Chen, R.; Li, T.; Xu, L.; Mai, L. New Insights into Phase-Mechanism Relationship of Mg_x MnO_2 Nanowires in Aqueous Zinc-Ion Batteries. *Small* **2022**, *18*, 2107743. [CrossRef] [PubMed]
34. Chong, Y.; Ning, J.; Min, S.; Ye, J.; Ge, C. Emerging nanozymes for potentiating radiotherapy and radiation protection. *Chin. Chem. Lett.* **2022**, *33*, 3315–3324. [CrossRef]
35. Feng, N.; Liu, Y.; Dai, X.; Wang, Y.; Guo, Q.; Li, Q. Advanced applications of cerium oxide based nanozymes in cancer. *RSC Adv.* **2022**, *12*, 1486–1493. [CrossRef]
36. Huang, Y.; Mu, X.; Wang, J.; Wang, Y.; Xie, J.; Ying, R.; Su, E. The recent development of nanozymes for food quality and safety detection. *J. Mater. Chem. B* **2022**, *10*, 1359–1368. [CrossRef]
37. Ren, X.; Chen, D.; Wang, Y.; Li, H.; Zhang, Y.; Chen, H.; Li, X.; Huo, M. Nanozymes-recent development and biomedical applications. *J. Nanobiotechnology* **2022**, *20*, 92. [CrossRef] [PubMed]
38. Wang, Q.; Jiang, J.; Gao, L. Catalytic antimicrobial therapy using nanozymes. *WIREs Nanomed. Nanobiotech.* **2022**, *14*, e.1769. [CrossRef]
39. Zandieh, M.; Liu, J. Surface Science of Nanozymes and Defining a Nanozyme Unit. *Langmuir* **2022**, *38*, 3617–3622. [CrossRef]

40. Da Costa, F.P.; Cipolatti, E.P.; Junior, A.F.; Henriques, R.O. Nanoflowers: A New Approach of Enzyme Immobilization. *Chem. Rec.* **2022**, *22*, e202100293. [CrossRef] [PubMed]
41. Demirbas, A. Comparison Study of Synthesized Red (or Blood) Orange Peels and Juice Extract-Nanoflowers and Their Antimicrobial Properties on Fish Pathogen (*Yersinia ruckeri*). *Indian J. Microbiol.* **2021**, *61*, 324–330. [CrossRef]
42. Li, Z.; Deng, S.; Yu, H.; Yin, Z.; Qi, S.; Yang, L.; Lv, J.; Sun, Z.; Zhang, M. Fe–Co–Ni trimetallic organic framework chrysanthemum-like nanoflowers: Efficient and durable oxygen evolution electrocatalysts. *J. Mater. Chem. A* **2022**, *10*, 4230–4241. [CrossRef]
43. Ouyang, Q.; Liu, K.; Zhu, Q.; Deng, H.; Le, Y.; Ouyang, W.; Yan, X.; Zhou, W.; Tong, J. Brain-Penetration and Neuron-Targeting DNA Nanoflowers Co-Delivering miR-124 and Rutin for Synergistic Therapy of Alzheimer's Disease. *Small* **2022**, *18*, 2107534. [CrossRef] [PubMed]
44. Yilmaz, S.G.; Demirbas, A.; Karaagac, Z.; Dadi, S.; Celik, C.; Yusufbeyoglu, S.; Ildiz, N.; Mandal, A.K.; Cimen, B.; Ocsoy, I. Synthesis of taurine-$Cu_3(PO_4)_2$ hybrid nanoflower and their peroxidase-mimic and antimicrobial properties. *J. Biotechnol.* **2022**, *343*, 96–101. [CrossRef] [PubMed]
45. Zhi, L.; Tu, J.; Li, J.; Li, M.; Liu, J. 3D holey hierarchical nanoflowers assembled by cobalt phosphide embedded N-doped carbon nanosheets as bifunctional electrocatalyst for highly efficient overall water splitting. *J. Colloid Interface Sci.* **2022**, *616*, 379–388. [CrossRef] [PubMed]
46. Du, J.; Liu, Z.; Li, Z.; Han, B.; Sun, Z.; Huang, Y. Carbon nanoflowers synthesized by a reduction–pyrolysis–catalysis route. *Mater. Lett.* **2005**, *59*, 456–458. [CrossRef]
47. Ma, X.; Yuan, B. Fabrication of carbon nanoflowers by plasma-enhanced chemical vapor deposition. *Appl. Surf. Sci.* **2009**, *255*, 7846–7850. [CrossRef]
48. Thongtem, S.; Singjai, P.; Thongtem, T.; Preyachoti, S. Growth of carbon nanoflowers on glass slides using sparked iron as a catalyst. *Mater. Sci. Eng. A Struct. Mater.* **2006**, *423*, 209–213. [CrossRef]
49. Bian, J.; Shu, S.; Li, J.; Huang, C.; Li, Y.Y.; Zhang, R.-Q. Reproducible and recyclable SERS substrates: Flower-like Ag structures with concave surfaces formed by electrodeposition. *Appl. Surf. Sci.* **2015**, *333*, 126–133. [CrossRef]
50. Cha, S.I.; Mo, C.B.; Kim, K.T.; Hong, S.H. Ferromagnetic Cobalt Nanodots, Nanorices, Nanowires and Nanoflowers by Polyol Process. *J. Mater. Res.* **2005**, *20*, 2148–2153. [CrossRef]
51. Wang, Z.; Zhang, J.; Ekman, J.M.; Kenis, P.J.A.; Lu, Y. DNA-Mediated Control of Metal Nanoparticle Shape: One-Pot Synthesis and Cellular Uptake of Highly Stable and Functional Gold Nanoflowers. *Nano Lett.* **2010**, *10*, 1886–1891. [CrossRef]
52. Bin, D.; Yang, B.; Zhang, K.; Wang, C.; Wang, J.; Zhong, J.; Feng, Y.; Guo, J.; Du, Y. Design of PdAg Hollow Nanoflowers through Galvanic Replacement and Their Application for Ethanol Electrooxidation. *Chem. A Eur. J.* **2016**, *22*, 16642–16647. [CrossRef] [PubMed]
53. Liu, L.J.; Guan, J.G.; Shi, W.D.; Sun, Z.G.; Zhao, J.S. Facile Synthesis and Growth Mechanism of Flowerlike Ni−Fe Alloy Nanostructures. *J. Phys. Chem. C Nanomater. Interfaces* **2010**, *114*, 13565–13570. [CrossRef]
54. Heli, H.; Rahi, A. Synthesis and Applications of Nanoflowers. *Recent Pat. Nanotechnol.* **2016**, *10*, 86–115. [CrossRef] [PubMed]
55. Kharisov, B.I. A Review for Synthesis of Nanoflowers. *Recent Pat. Nanotechnol.* **2008**, *2*, 190–200. [CrossRef]
56. Kim, S.-I.; Lee, J.-S.; Ahn, H.-J.; Song, H.-K.; Jang, J.-H. Facile Route to an Efficient NiO Supercapacitor with a Three-Dimensional Nanonetwork Morphology. *ACS Appl. Mater. Interfaces* **2013**, *5*, 1596–1603. [CrossRef]
57. Bai, Z.; Yan, X.; Li, Y.; Kang, Z.; Cao, S.; Zhang, Y. 3D-Branched ZnO/CdS Nanowire Arrays for Solar Water Splitting and the Service Safety Research. *Adv. Energy Mater.* **2016**, *6*, 1501459. [CrossRef]
58. Hu, Z.; Wang, L.; Zhang, K.; Wang, J.; Cheng, F.; Tao, Z.; Chen, J. MoS_2Nanoflowers with Expanded Interlayers as High-Performance Anodes for Sodium-Ion Batteries. *Angew. Chem. Int. Ed. Engl.* **2014**, *53*, 12794–12798. [CrossRef] [PubMed]
59. Leung, K.C.-F.; Xuan, S.; Zhu, X.; Wang, D.; Chak, C.-P.; Lee, S.-F.; Ho, W.K.-W.; Chung, B.C.-T. Gold and iron oxide hybrid nanocomposite materials. *Chem. Soc. Rev.* **2012**, *41*, 1911–1928. [CrossRef] [PubMed]
60. Ma, C.-B.; Qi, X.; Chen, B.; Bao, S.; Yin, Z.; Wu, X.-J.; Luo, Z.; Wei, J.; Zhang, H.-L.; Zhang, H. MoS2 nanoflower-decorated reduced graphene oxide paper for high-performance hydrogen evolution reaction. *Nanoscale* **2014**, *6*, 5624–5629. [CrossRef] [PubMed]
61. Mohanty, A.; Garg, N.; Jin, R. A Universal Approach to the Synthesis of Noble Metal Nanodendrites and Their Catalytic Properties. *Angew. Chem. Int. Ed. Engl.* **2010**, *49*, 4962–4966. [CrossRef]
62. Arya, S.K.; Saha, S.; Ramirez-Vick, J.E.; Gupta, V.; Bhansali, S.; Singh, S.P. Recent advances in ZnO nanostructures and thin films for biosensor applications: Review. *Anal. Chim. Acta* **2012**, *737*, 1–21. [CrossRef]
63. He, S.; Hu, C.; Hou, H.; Chen, W. Ultrathin MnO2 nanosheets supported on cellulose based carbon papers for high-power supercapacitors. *J. Power Sources* **2014**, *246*, 754–761. [CrossRef]
64. Hu, L.; Ren, Y.; Yang, H.; Xu, Q. Fabrication of 3D Hierarchical MoS_2/Polyaniline and MoS_2/C Architectures for Lithium-Ion Battery Applications. *ACS Appl. Mater. Interfaces* **2014**, *6*, 14644–14652. [CrossRef]
65. Huang, Y.; Ran, X.; Lin, Y.; Ren, J.; Qu, X. Self-assembly of an organic–inorganic hybrid nanoflower as an efficient biomimetic catalyst for self-activated tandem reactions. *Chem. Commun.* **2015**, *51*, 4386–4389. [CrossRef]
66. Liu, Y.; Jiao, Y.; Zhang, Z.; Qu, F.; Umar, A.; Wu, X. Hierarchical SnO_2 Nanostructures Made of Intermingled Ultrathin Nanosheets for Environmental Remediation, Smart Gas Sensor, and Supercapacitor Applications. *ACS Appl. Mater. Interfaces* **2014**, *6*, 2174–2184. [CrossRef] [PubMed]
67. Wang, D.; Pan, Z.; Wu, Z.; Wang, Z.; Liu, Z. Hydrothermal synthesis of MoS_2 nanoflowers as highly efficient hydrogen evolution reaction catalysts. *J. Power Sources* **2014**, *264*, 229–234. [CrossRef]

68. Yang, W.; Gao, Z.; Wang, J.; Ma, J.; Zhang, M.; Liu, L. Solvothermal One-Step Synthesis of Ni–Al Layered Double Hydroxide/Carbon Nanotube/Reduced Graphene Oxide Sheet Ternary Nanocomposite with Ultrahigh Capacitance for Supercapacitors. *ACS Appl. Mater. Interfaces* **2013**, *5*, 5443–5454. [CrossRef]
69. Zeng, M.; Li, Y.; Liu, F.; Yang, Y.; Mao, M.; Zhao, X. Cu doped OL-1 nanoflower: A UV–vis-infrared light-driven catalyst for gas-phase environmental purification with very high efficiency. *Appl. Catal. B* **2017**, *200*, 521–529. [CrossRef]
70. Xiao, N.; Venton, B.J. Rapid, Sensitive Detection of Neurotransmitters at Microelectrodes Modified with Self-assembled SWCNT Forests. *Anal. Chem.* **2012**, *84*, 7816–7822. [CrossRef] [PubMed]
71. Yao, H.-B.; Fang, H.-Y.; Wang, X.-H.; Yu, S.-H. Hierarchical assembly of micro-/nano-building blocks: Bio-inspired rigid structural functional materials. *Chem. Soc. Rev.* **2011**, *40*, 3764–3785. [CrossRef] [PubMed]
72. Zan, G.; Wu, Q. Biomimetic and Bioinspired Synthesis of Nanomaterials/Nanostructures. *Adv. Mater.* **2016**, *28*, 2099–2147. [CrossRef]
73. Altinkaynak, C.; Tavlasoglu, S.; Ÿzdemir, N.; Ocsoy, I. A new generation approach in enzyme immobilization: Organic-inorganic hybrid nanoflowers with enhanced catalytic activity and stability. *Enzym. Microb. Technol.* **2016**, *93–94*, 105–112. [CrossRef]
74. Lin, Z.; Xiao, Y.; Wang, L.; Yin, Y.; Zheng, J.; Yang, H.; Chen, G. Facile synthesis of enzyme—Inorganic hybrid nanoflowers and their application as an immobilized trypsin reactor for highly efficient protein digestion. *RSC Adv.* **2014**, *4*, 13888–13891. [CrossRef]
75. Lin, Z.; Xiao, Y.; Yin, Y.; Hu, W.; Liu, W.; Yang, H. Facile Synthesis of Enzyme-Inorganic Hybrid Nanoflowers and Its Application as a Colorimetric Platform for Visual Detection of Hydrogen Peroxide and Phenol. *ACS Appl. Mater. Interfaces* **2014**, *6*, 10775–10782. [CrossRef] [PubMed]
76. Nadar, S.S.; Gawas, S.D.; Rathod, V.K. Self-assembled organic-inorganic hybrid glucoamylase nanoflowers with enhanced activity and stability. *Int. J. Biol. Macromol.* **2016**, *92*, 660–669. [CrossRef]
77. Sun, J.; Ge, J.; Liu, W.; Lan, M.; Zhang, H.; Wang, P.; Wang, Y.; Niu, Z. Multi-enzyme co-embedded organic–inorganic hybrid nanoflowers: Synthesis and application as a colorimetric sensor. *Nanoscale* **2014**, *6*, 255–262. [CrossRef] [PubMed]
78. Yin, Y.; Xiao, Y.; Lin, G.; Xiao, Q.; Lin, Z.; Cai, Z. An enzyme–inorganic hybrid nanoflower based immobilized enzyme reactor with enhanced enzymatic activity. *J. Mater. Chem. B* **2015**, *3*, 2295–2300. [CrossRef]
79. Kim, K.H.; Jeong, J.-M.; Lee, S.J.; Choi, B.G.; Lee, K.G. Protein-directed assembly of cobalt phosphate hybrid nanoflowers. *J. Colloid Interface Sci.* **2016**, *484*, 44–50. [CrossRef] [PubMed]
80. Wu, Z.-F.; Wang, Z.; Zhang, Y.; Ma, Y.-L.; He, C.-Y.; Li, H.; Chen, L.; Huo, Q.-S.; Wang, L.; Li, Z.-Q. Amino acids-incorporated nanoflowers with an intrinsic peroxidase-like activity. *Sci. Rep.* **2016**, *6*, 22412. [CrossRef]
81. Ge, J.; Lei, J.; Zare, R.N. Protein–inorganic hybrid nanoflowers. *Nat. Nanotechnol.* **2012**, *7*, 428–432. [CrossRef] [PubMed]
82. Wang, L.-B.; Wang, Y.-C.; He, R.; Zhuang, A.; Wang, X.; Zeng, J.; Hou, J.G. A New Nanobiocatalytic System Based on Allosteric Effect with Dramatically Enhanced Enzymatic Performance. *J. Am. Chem. Soc.* **2013**, *135*, 1272–1275. [CrossRef]
83. Qiao, Y.; Lin, Y.; Wang, Y.; Yang, Z.; Liu, J.; Zhou, J.; Yan, Y.; Huang, J. Metal-Driven Hierarchical Self-Assembled One-Dimensional Nanohelices. *Nano Lett.* **2009**, *9*, 4500–4504. [CrossRef]
84. Qiao, Y.; Wang, Y.; Yang, Z.; Lin, Y.; Huang, J. Self-templating of metal-driven supramolecular self-assembly: A general ap-proach toward 1D inorganic nanotubes. *Chem. Mater.* **2011**, *23*, 1182–1187. [CrossRef]
85. Uras, I.S.; Ebada, S.S.; Korinek, M.; Albohy, A.; Abdulrazik, B.S.; Wang, Y.-H.; Chen, B.-H.; Horng, J.-T.; Lin, W.; Hwang, T.-L.; et al. Anti-Inflammatory, Antiallergic, and COVID-19 Main Protease (Mpro) Inhibitory Activities of Butenolides from a Ma-rine-Derived Fungus *Aspergillus terreus*. *Molecules* **2021**, *26*, 3354. [CrossRef] [PubMed]
86. Yu, Y.; Fei, X.; Tian, J.; Xu, L.; Wang, X.; Wang, Y. Self-assembled enzyme–inorganic hybrid nanoflowers and their application to enzyme purification. *Colloids Surf. B Biointerfaces* **2015**, *130*, 299–304. [CrossRef]
87. Nitta, K.; Fujita, N.; Yoshimura, T.; Arai, K.; Yamamoto, Y. Metabolic products of *Aspergillus terreus*. IX. Biosynthesis of butyrolactone derivatives isolated from strains IFO 8835 and 4100. *Chem. Pharm. Bull.* **1983**, *31*, 1528–1533. [CrossRef]
88. Bauer, A.W.; Kirby, W.M.; Sherris, J.C.; Turck, M. Antibiotic susceptibility testing by a standardized single disk method. *Am. J. Clin. Pathol.* **1966**, *45*, 493–496. [CrossRef]
89. Ildiz, N.; Baldemir, A.; Altinkaynak, C.; Özdemir, N.; Yilmaz, V.; Ocsoy, I. Self assembled snowball-like hybrid nanostructures comprising *Viburnum opulus* L. extract and metal ions for antimicrobial and catalytic applications. *Enzym. Microb. Technol.* **2017**, *102*, 60–66. [CrossRef] [PubMed]
90. Koca, F.D. Preparation of thymol incorporated organic-inorganic hybrid nanoflowers as a novel fenton agent with in-trinsic catalytic and antimicrobial activities. *Inorg. Nano-Met. Chem.* **2022**, *52*, 322–327. [CrossRef]
91. Altinkaynak, C.; Yilmaz, I.; Koksal, Z.; Özdemir, H.; Ocsoy, I.; Özdemir, N. Preparation of lactoperoxidase incorporated hybrid nanoflower and its excellent activity and stability. *Int. J. Biol. Macromol.* **2016**, *84*, 402–409. [CrossRef] [PubMed]
92. Ariza-Avidad, M.; Salinas-Castillo, A.; Capitán-Vallvey, L. A 3D μPAD based on a multi-enzyme organic–inorganic hybrid nanoflower reactor. *Biosens. Bioelectron.* **2016**, *77*, 51–55. [CrossRef] [PubMed]
93. Huang, K.-J.; Liu, Y.-J.; Liu, Y.-M.; Wang, L.-L. Molybdenum disulfide nanoflower-chitosan-Au nanoparticles composites based electrochemical sensing platform for bisphenol A determination. *J. Hazard. Mater.* **2014**, *276*, 207–215. [CrossRef]
94. Liang, L.; Fei, X.; Li, Y.; Tian, J.; Xu, L.; Wang, X.; Wang, Y. Hierarchical assembly of enzyme-inorganic composite materials with extremely high enzyme activity. *RSC Adv.* **2015**, *5*, 96997–97002. [CrossRef]

95. Somturk, B.; Hancer, M.; Ocsoy, I.; Özdemir, N. Synthesis of copper ion incorporated horseradish peroxidase-based hybrid nanoflowers for enhanced catalytic activity and stability. *Dalton Trans.* **2015**, *44*, 13845–13852. [CrossRef]
96. Thawari, A.G.; Rao, C.P. Peroxidase-like Catalytic Activity of Copper-Mediated Protein–Inorganic Hybrid Nanoflowers and Nanofibers of β-Lactoglobulin and α-Lactalbumin: Synthesis, Spectral Characterization, Microscopic Features, and Catalytic Activity. *ACS Appl. Mater. Interfaces* **2016**, *8*, 10392–10402. [CrossRef]
97. Zhang, Z.; Kong, X.-Y.; Xiao, K.; Xie, G.; Liu, Q.; Tian, Y.; Zhang, H.; Ma, J.; Wen, L.; Jiang, L. A Bioinspired Multifunctional Heterogeneous Membrane with Ultrahigh Ionic Rectification and Highly Efficient Selective Ionic Gating. *Adv. Mater.* **2016**, *28*, 144–150. [CrossRef] [PubMed]
98. Mutti, F.; Fuchs, C.; Pressnitz, D.; Sattler, J.; Kroutil, W. Stereoselectivity of four (R)-selective transaminases for the asymmetric amination of ketones. *Adv. Synth. Catal.* **2011**, *353*, 3227–3233. [CrossRef]
99. Łyskowski, A.; Gruber, C.; Steinkellner, G.; Schürmann, M.; Schwab, H.; Gruber, K.; Steiner, K. Crystal Structure of an (R)-Selective ω-Transaminase from *Aspergillus terreus*. *PLoS ONE* **2014**, *9*, e87350. [CrossRef] [PubMed]
100. Li, G.; He, D.; Qian, Y.; Guan, B.; Gao, S.; Cui, Y.; Yokoyama, K.; Wang, L. Fungus-Mediated Green Synthesis of Silver Nanoparticles Using *Aspergillus terreus*. *Int. J. Mol. Sci.* **2012**, *13*, 466–476. [CrossRef]
101. Bunbamrung, N.; Intaraudom, C.; Dramae, A.; Komwijit, S.; Laorob, T.; Khamsaeng, S.; Pittayakhajonwut, P. Antimicrobial, antimalarial and anticholinesterase substances from the marine-derived fungus Aspergillus terreus BCC51799. *Tetrahedron* **2020**, *76*, 131496. [CrossRef]
102. Jain, P.; Pundir, R.K. Effect of different carbon and nitrogen sources on *Aspergillus terreus* antimicrobial metabolite pro-duction. *Int. J. Pharm. Sci. Rev. Res.* **2010**, 5.
103. San-Martín, A.; Rovirosa, J.; Vaca, I.; Vergara, K.; Acevedo, L.; Viña, D.; Orallo, F.; Chamy, M.C. New butyrolactone from a marine-derived fungus *Aspergillus* sp. *J. Chil. Chem. Soc.* **2011**, *56*, 625–627. [CrossRef]
104. Klančnik, A.; Piskernik, S.; Jeršek, B.; Možina, S.S. Evaluation of diffusion and dilution methods to determine the antibacterial activity of plant extracts. *J. Microbiol. Methods* **2010**, *81*, 121–126. [CrossRef] [PubMed]